

Experimental Study and Response Surface Methodology of Azo Dye as an Eco-Friendly Corrosion Inhibitor for Stainless Steel in a Chloride Solution

Fidelis Ebunta Abeng

*Department of Chemistry, Materials and Electrochemistry Research Group, University of
Cross River State, P. O. Box 1123, Calabar, Nigeria*

fidelisebuna@unicross.edu.ng

Received 01/05/2023; accepted 05/07/2023

<https://doi.org/10.4152/pea.2024420603>

Abstract

DAD was investigated as CI for SS corrosion in a 3.5% NaCl solution, using WL, thermometric and RSM techniques. The analyses results show that IE(%) of DAD was dependent on its Ct and T. The highest IE(%) values were recorded on 5.0 g/L, at 303 K, by thermometric and WL methods (90.0 and 98%, respectively). DAD adsorption onto the SS surface was found to be spontaneous, obeyed Langmuir's isotherm, and its mechanism appeared to be partly physical, partly chemical. The results of RSM techniques supported experimental data. Finally, SEM was used to examine SS surfaces morphology without and with DAD, and its results confirmed the CI process.

Keywords: adsorption; corrosion; DAD; NaCl; RSM; SEM; SS; WL.

Introduction*

SS is a metallic material usually employed in many different fields, including architecture, building and chemical engineering, metals extraction, desalination and wastewater treatment facilities, oil and gas industry, transportation, aerospace, food and beverage sectors, due to its great corrosion resistance [1]. Cr in SS produces a passive film layer of Cr-rich oxide at lower T, in O presence, which is what gives the material its high resistance [1-2]. During SS maintenance procedures employed in most manufacturing industries, saline media is used to clean steel parts and remove rust and calcification, sometimes in acid and alkali presence [3]. The disadvantage of this essential procedure is alkali corrosive attack on the metal surface, which results in failings, or even long-term damage to machine parts.

* The abbreviations and symbols definition lists are in page 430.

CI are chemicals substances added to alkaline solutions to minimize corrosion. CI primary mechanism occurs through their molecule's adsorption onto the metal surface. Due to this process, water molecules are displaced, and a barrier that shields the metal surface from aggressive media is created. Thus, it is important to consider the variables that influence the adsorption level. The presence of heteroatoms and specific functional groups, and the availability of conjugated electrons are all factors that provide adsorption centres for inhibitor molecules to bind with the metal surface via physisorption and/or chemisorption processes. Organic compounds must meet these structural requirements to be effective CI. The solution T and the inhibitors Ct are other variables that significantly impact adsorption.

It is known that the substructures of several regularly used dyes are organic inhibitors and share significant similarities with most heterocyclic organic compounds like pyridines, furans, imidazoles, thiophenes and isoxazoles [3-7].

This characteristic has inspired scientists throughout the world to investigate the use of dyes as CI. Dyes have started to replace harmful CI that were previously used, because they are non-toxic and have a negative influence on the environment.

Azo dyes are amino based aromatic compounds. Literature has reported studies on the extensive use of amine-based aromatic compounds as CI for several metals and alloys in various electrolytes. Generally, the amino group (-NH₂) of such compounds serves as a site for interaction with the metallic surface, and the remaining molecules behave as water repellent [8].

[9] synthesized and characterized a novel coumarin azo dye as CI for MS in an acidic environment, applying both experimental and theoretical approaches. Their findings show that the dye inhibited the corrosion process and protected the MS surface. Table 1 lists other research on similar dyes.

Table 1: Works related to the present research on different metals and corrosive media.

| Metals | Inhibitors | Corrosive media | IE(%) | Ref. |
|--------|--|--------------------------------|----------------|------------|
| MS | Azo dye compound | HCl | 96% | [18] |
| MS | [N-substituted p-amino azo benzene] | H ₂ SO ₄ | 82.48% | [19] |
| Al | Mono azo dyes | NaOH | 73% | [20] |
| MS | Mordant green 17 | HCl | 83.1% | [21] |
| CS | Benzonitrile azo dye | HCl | 99.5% | [22] |
| CS | Azo chromoto tropic acid dye | H ₂ SO ₄ | 82.3% | [23] |
| CS | Alizarin yellow dye | HCl | 97.3% | [24] |
| MS | Allura red, sunset yellow and amaranth | H ₂ SO ₄ | 90, 80 and 78% | [25] |
| MS | Chromotropic acid dye and | H ₂ SO ₄ | 83 and 87% | [26] |
| SS | DAD | NaCl | 90-98% | This study |

In the present study, DAD was investigated as CI for SS immersed in NaCl. Fig. 1 depicts DAD molecular structure. In addition to its eco-friendliness and availability, the molecule is relatively bulky and rich in N heteroatoms, making it a promising adsorbate and, hence, a viable candidate for CI [10].

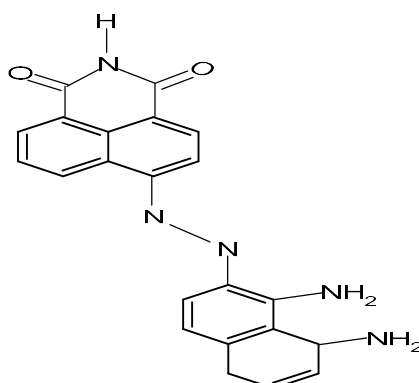


Figure 1: DAD molecular structure.

DAD molecular structure qualifies it as a suitable CI for two reasons: there are numerous N and O heteroatoms in its chemical structure, which have been widely discovered and proved in literature as excellent sites for adsorption onto the metal surface [11]. DAD has also a very high molecular weight. Literature has widely reported that IE(%) is higher as the molecular species mass increases. This phenomenon is often due to the inhibitor bulkiness, which increases the metal SC [11].

Corrosion and inhibiting processes have been investigated by several authors who have employed thermometric and RSM methods, which are vital in estimating and predicting the service life span of metals in real-world settings and are less time consuming [12-17]. However, DAD effects on SS corrosion behaviour are not yet well understood, and the use of RSM for predicting the inhibitor effect on SS in Cl media has not yet been reported until now.

Therefore, herein, experimental validation was done with the projected ideal process parameters, and the related IE(%) was examined using WL and thermometric methods, which are less expensive and quicker [10].

Experimental

Sample material and inhibitor preparation

In this study, a grade SS-410 SS sample with a thickness of 0.5 cm was employed, and it was cut into coupons of 5 x 1.5 cm. A 0.35 cm hole was drilled on each coupon. A twine was passed through this hole to aid suspension and total immersion in the media during WL measurements. SS-410 SS specimen chemical composition was: Cr (11.14%), Mn (0.82%), Cu (0.43%), C (0.134%), P (0.02%), Si (0.005%) and the remain Fe [2]. DAD was purchased from Sigma Aldrich chemicals and used without further purification. 3.5% NaCl was prepared and used for making the test solution with DAD. To prepare 5.0 g/L Ct of the inhibitor stock solution, 5.0 g/L DAD were dissolved in 1000 mL 3.5% NaCl solution. Then, the resulting solution was allowed to stand for 24 h, to enhance DAD solubility. Different Ct of DAD were calculated from the stock solution, using the dilution formula $C_1V_1 = C_2V_2$, and subsequently used in experimental measurements.

WL test

WL approach is the one that is most frequently used to evaluate CI, since it is quite easy and dependable. Many corrosion monitoring methods use WL as a foundational method. Herein, the SS surface was polished to a mirror shine using 1200 and 800 grit emery paper, then washed with distilled water, rinsed with acetone, and finally dried in a desiccator, before being submerged in the test solution (250 mL). WL experiment was carried out by SS total immersion in a 3.5% NaCl solution with and without DAD. The specimens were removed from the solution after 24 h, washed with a bristle brush under running tap water, for removing the corrosion product, dried in a desiccator, and reweighed precisely. WL of SS was determined by the difference between initial and final weights. For each solution, experiments were conducted thrice. The mean value was then recorded and used to calculate CR and SC [18-27].

Thermometric test

A calorimeter was used to perform thermometric test. The principle behind this technique is to monitor the change in T per min. This experiment was carried out at 30 and 60 °C. IE(%) was evaluated from RN obtained in Eq. 1.

$$RN = \frac{T_m - T_i}{t} \quad (1)$$

where T_m and T_i are maximum and initial T in °C, and t is the time taken in min to reach maximum T.

$$IE\% = \frac{RN_{Blank} - RN_{Inhi}}{RN_{Blank}} \times 100 \quad (2)$$

where RN_{blank} and RN_{inhi} are RN for SS corrosion in an aqueous solution without and with inhibitor, respectively.

RSM

For the data modelling and experimental runs, Design-Expert 13 software was employed. According to Table 2, the variables investigated were IT (A), T (B) and inhibitor Ct (C) (multiple input).

Table 2: CCD factor levels of independent variables.

| Independent variable | Low factor level | Medium factor level | High factor level |
|----------------------|------------------|---------------------|-------------------|
| A: IT (h) | 24.0 | 72.0 | 120.0 |
| B: T (°C) | 25.0 | 28.0 | 30.0 |
| C: Ct of DAD (g/L) | 0.1 | 2.6 | 5.0 |

Three levels of analysis were done on these 3 variables. To decide where the experimental run would take place, CCD was used in the trial design. 16 experimental runs were produced using CCD. The studies were conducted in random order, to prevent systematic errors. RSM results were assessed. The experimental evaluation of the various effects on CI at the design locations was carried out. A mathematical model was developed, for representing the relationship

between process factors and IE(%). Using RSM, one may predict the optimum value for the highest possible IE(%).

ANOVA and graphical analysis of IE(%) and CR were obtained from RSM, after responses evaluation (Table 3).

Table 3: ANOVA for CI of SS in 3. 5% NaCl with DAD.

| ANOVA for RSM quadratic model [partial sum of squares - Type III] | | | | | | |
|--|----------------|----|-------------|----------------------|-------------------|--------------|
| Source | Sum of squares | Df | Mean square | F-value | P-value, Prob > F | |
| Model | 9814.19 | 9 | 1090.47 | 41.48 | 0.0001 | Significant* |
| A-IT | 3120 | 1 | 3120 | 15.1 | 1.0000 | |
| B-T | 8011.32 | 1 | 8011.32 | 304.71 | <0.0001 | |
| C- DAD | 232 | 1 | 232 | 45.3 | 1.0000 | |
| AB | 18 | 1 | 18 | 2.7 | 1.0000 | |
| AC | 7 | 1 | 7 | 0.52 | 1.0000 | |
| BC | 4.3 | 1 | 4.3 | 0.38 | 1.0000 | |
| A ² | 15.26 | 1 | 15.26 | 0.5804 | 0.4750 | |
| B ² | 1511.65 | 1 | 1511.65 | 57.50 | 0.0003 | |
| C ² | 15.26 | 1 | 15.26 | 0.5804 | 0.4750 | |
| Residual | 157.75 | 6 | 26.29 | | | |
| Lack of fit | 157.75 | 5 | 31.55 | | | |
| Pure error | 0.0000 | 1 | 0.0000 | | | |
| Cor total | 9971.94 | 15 | | | | |
| STD | | | | R ² | 0.9842 | |
| Mean | | | | Adj. R ² | 0.9605 | |
| CV% | | | | Pred. R ² | 0.8802 | |
| Press | | | | Adeq. precision | 1194.58 | |

It was also possible to derive mathematical models in terms of coded factors, which enabled to predict responses for a given level of each factor [28-30].

Results and discussion

WL measurement

Fig. 2a displays calculated WL plots of SS in a 3.5% NaCl solution with and without various Ct of DAD, at 30 °C. WL of SS decreased with higher Ct of DAD. This means that DAD inhibited SS corrosion in a NaCl solution. WL of SS was calculated by eq. (3).

$$\Delta M = \frac{m_1 - m_2}{At} \quad (3)$$

where m_1 and m_2 are WL of SS specimens before and after their immersion in NaCl. Eq. 4 was used to calculate SC on SS.

$$\theta = \frac{1 - CR_{inh}}{CR_{blank}} \quad (4)$$

where θ is SC of SS by DAD, and CR_{inh} and CR_{blank} are CR values of SS without and with DAD, respectively. They were obtained from the slopes plotted in Figs. 2a and b. SC on SS by DAD in an aqueous medium depends on the inhibitor Ct, due to its adsorption onto the metal [31-32].

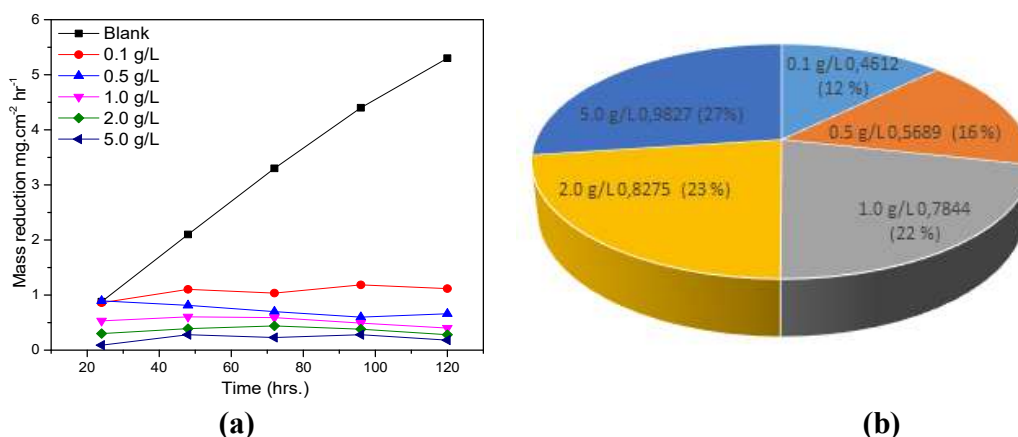


Figure 2: (a) IT-WL curves of SS in a 3.5% NaCl solution with and without DAD, in various Ct, at 30 °C; (b) chart showing SC of DAD on SS.

Thermometric measurement

Thermometric analysis has proven to be quite useful in the understanding of metal corrosion. The method can also be used to assess IE(%) of a variety of chemical substances. Figs. 3a and 3b depict T variation with IT, for SS corrosion in a 3.5% NaCl solution, without and with DAD, at various Ct. The system T rose progressively, due to the exothermic corrosion reaction. The blank solution RN, at 30 and 60 °C, was recorded as 0.8 and 1.40 °C/min⁻¹, respectively. Table 4 also shows that RN values decreased with a higher Ct of DAD. This was due to DAD adsorption onto the SS surface, which prevented its corrosion in Cl solutions [27, 33].

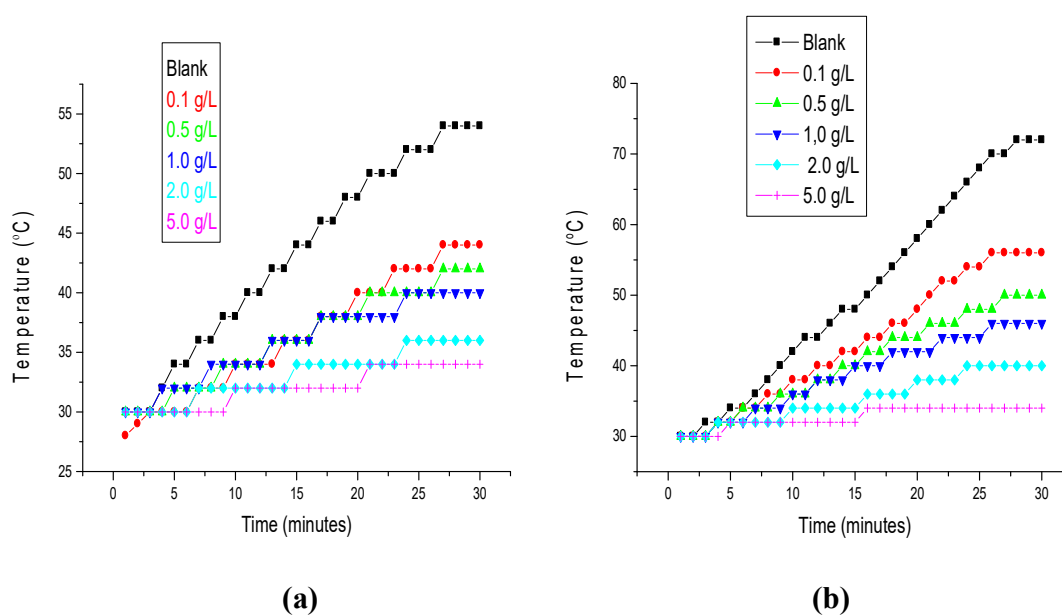


Figure 3: SS corrosion T-IT curves in 3.5% NaCl solutions without and with DAD, at various Ct.

Table 4: RN thermometric calculated values for SS corrosion in 3.5% NaCl with DAD.

| Ct | T | RN | SC | IE(%) |
|---------|-------|------|-------|-------|
| blank | | 0.80 | | |
| 0.1 g/L | 30 °C | 0.53 | 0.337 | 33.7 |
| 0.5 g/L | | 0.40 | 0.500 | 50.0 |
| 1.0 g/L | | 0.33 | 0.587 | 58.7 |
| 2.0 g/L | | 0.20 | 0.750 | 75.0 |
| 5.0 g/L | | 0.13 | 0.837 | 83.7 |
| blank | | 1.40 | | |
| 0.1 g/L | 60 °C | 0.93 | 0.385 | 38.5 |
| 0.5 g/L | | 0.66 | 0.528 | 52.8 |
| 1.0 g/L | | 0.53 | 0.621 | 62.1 |
| 2.0 g/L | | 0.40 | 0.764 | 76.4 |
| 5.0 g/L | | 0.20 | 0.907 | 90.7 |

Results of RSM analysis

Table 5 demonstrates how Ct, T and IT affected WL, CR and IE(%). An ideal IE(%) of 98% was attained.

Table 5: RSM results of SS corrosion in a 3.5% NaCl solution with DAD.

| Std. | Run | Factor 1 (A) IT (h) | Factor 2 (B)T (°C) | Factor 3 (C) Ct of DAD (g/L) | Response 1 WL (mg) | Response 2 CR (mg/cm ² /h) | Response 3 IE% |
|------|-----|------------------------|-----------------------|------------------------------------|-----------------------|---|-------------------|
| 14 | 1 | 72 | 28 | 5 | 0.4 | 0.511 | 98 |
| 15 | 2 | 72 | 28 | 2.6 | 0.4 | 0.511 | 72 |
| 2 | 3 | 120 | 26 | 0.1 | 0.215 | 3.256 | 24 |
| 11 | 4 | 72 | 25 | 2.6 | 0.03 | 3.256 | 72 |
| 7 | 5 | 24 | 30 | 5 | 0.215 | 6 | 98 |
| 4 | 6 | 120 | 30 | 0.1 | 0.4 | 0.511 | 24 |
| 8 | 7 | 120 | 30 | 5 | 0.03 | 7.87 | 98 |
| 1 | 8 | 24 | 26 | 0.1 | 0.4 | 6 | 24 |
| 6 | 9 | 120 | 26 | 5 | 0.03 | 0.5 | 98 |
| 16 | 10 | 72 | 28 | 2.6 | 0.03 | 3.256 | 72 |
| 12 | 11 | 72 | 30 | 2.6 | 0.215 | 3.256 | 72 |
| 3 | 12 | 24 | 30 | 0.1 | 0.03 | 0.511 | 24 |
| 10 | 13 | 72 | 28 | 2.6 | 0.215 | 6 | 72 |
| 9 | 14 | 24 | 28 | 2.6 | 0.215 | 6 | 72 |
| 13 | 15 | 72 | 28 | 5 | 0.215 | 3.256 | 98 |
| 5 | 16 | 24 | 26 | 5 | 0.53 | 3.256 | 98 |

Predicted and actual IE(%) values are shown in Fig. 4a, which indicates a strong correlation between experimental and theoretical studies. Eq. 5 is the general quadratic model with significant and insignificant variables, such as IT (A), T (B) and inhibitor Ct (C), which links them to IE(%). The model was reduced to Eq. 6, when only significant terms were taken into consideration. According to the statistical study, there was only a 0.01% chance that F-value could occur due to noise, and Ct of O and flow rates of DAD functional groups would be uncontrollable

sources of noise. The models are important and useful for navigating the design environment [34].

$$IE(\%) = +89.53 + 16A + 25B + 3C - 5.1AB - -5.0AC - 5.6BC - 1.28A^2 - 12.77B^2 - 1.28C^2 \quad (5)$$

$$IE(\%) = +89.53 + 16A + 25B + 3C - 1.28A^2 \quad (6)$$

RSM plots

Researchers were able to examine the interactive impact of process variables on the percentage IE(%), by plotting a three-dimensional surface curve against any two independent variables, while holding the other one constant. Fig. 4 describes predicted vs. experimental plots, demonstrating that they were properly distributed near the straight line. This indicates a strong relationship between experimental and predicted response values. It also confirms that the selected quadratic model could accurately predict response variables for experimental data. A linear graph showing the link between factors and DAD corrosion IE(%) response in the planned experiment was produced by predicted vs. experimental plots (Fig. 4). Figs. 5 to 7 illustrate the 3D surface plot.

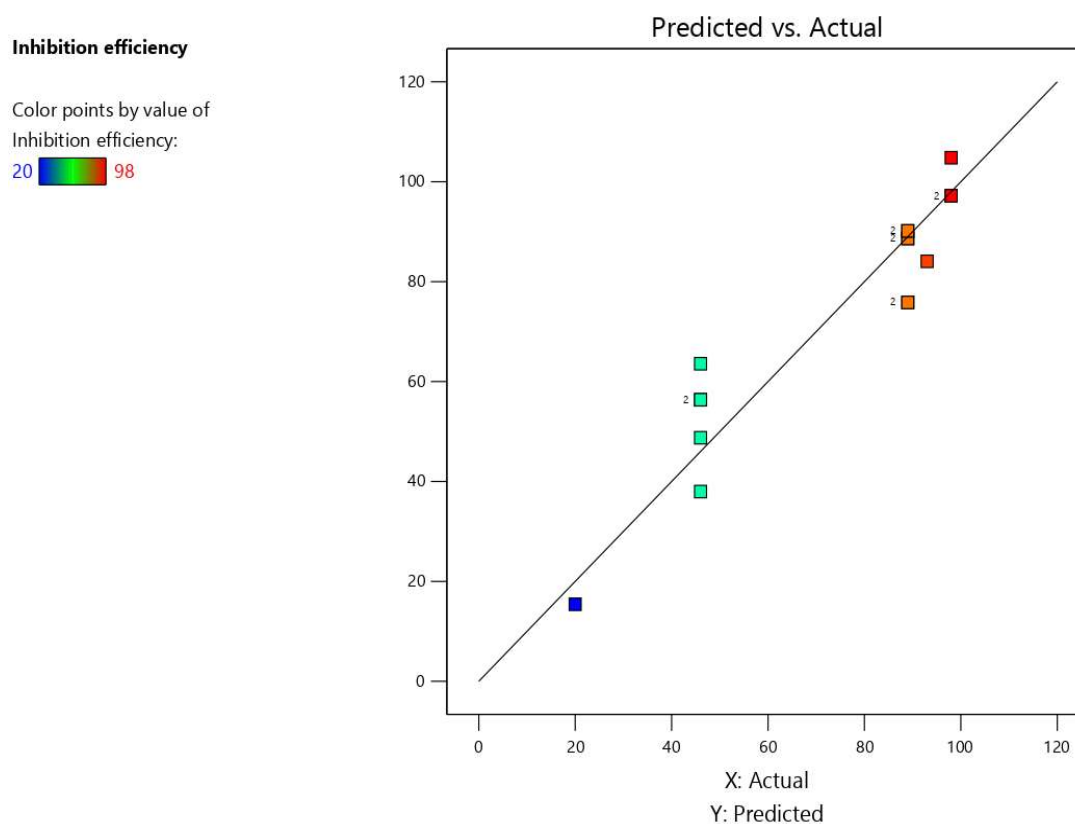


Figure 4: Plot comparing DAD predicted and experimental IE(%) values on SS corrosion in a 3.5% NaCl solution.

Fig. 5 shows that, with a given Ct of CI, IE(%) increases with IT, but decreases with higher T.

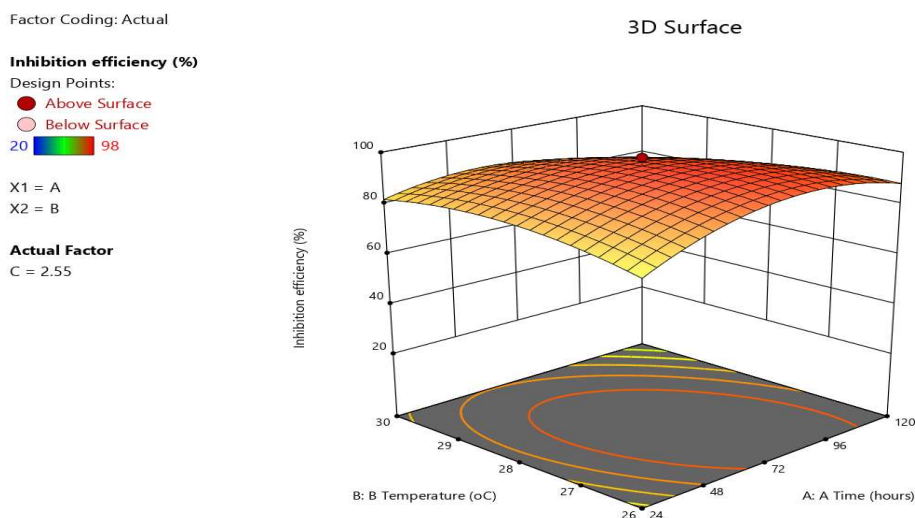


Figure 5: Effect of IT and T on DAD ability to inhibit SS corrosion in a 3.5% NaCl solution.

Fig. 6 reveals that CR decreased as Ct of DAD increased. However, CR increased with higher T. This confirms that the adsorption mechanism was physical, although Fig. 7 shows that WL decreased with higher Ct of DAD, and increased with prolonged IT [28-29, 34-35].

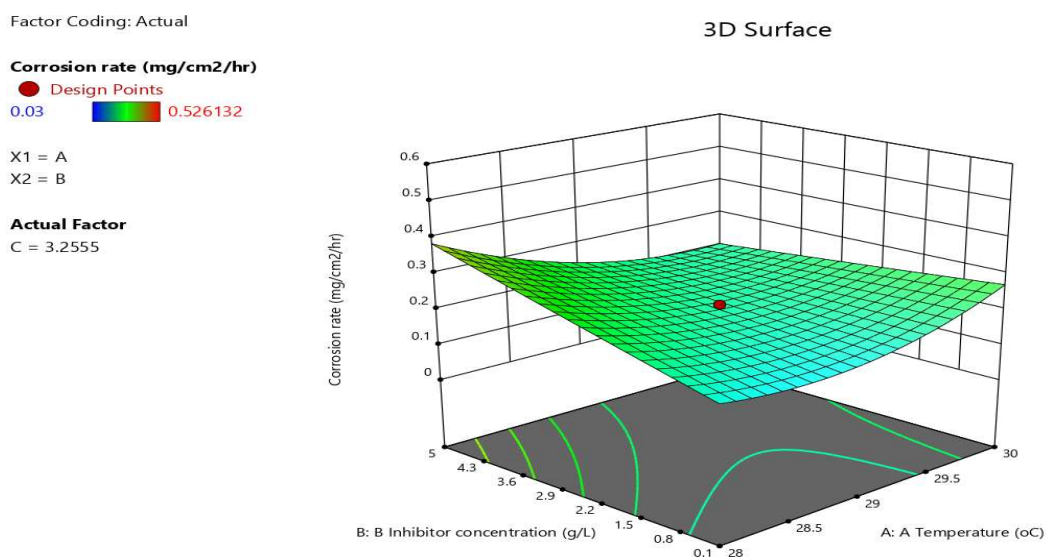


Figure 6: Effect of T and Ct of DAD on the CR of SS.

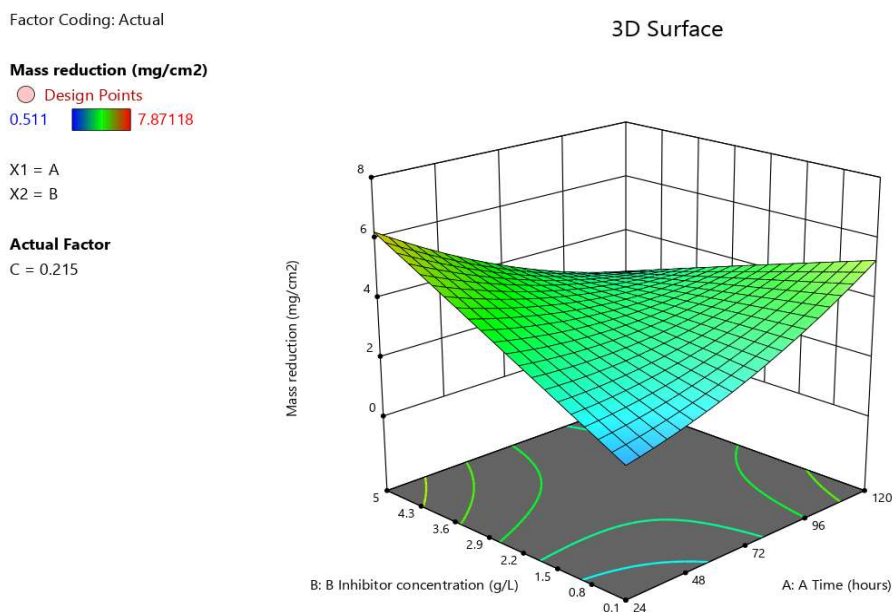


Figure 7: Effects of Ct of DAD and IT of SS on WL.

Adsorption isotherm

Langmuir’s isotherm, which is defined by Eq. (7), is one of the most common methods for determining the adsorption nature of a CI.

$$C/\theta = 1/K_{ads} + C \tag{7}$$

The plot of C/θ vs. C gave a linear plot with R² equal to 0.998 (Fig. 8).

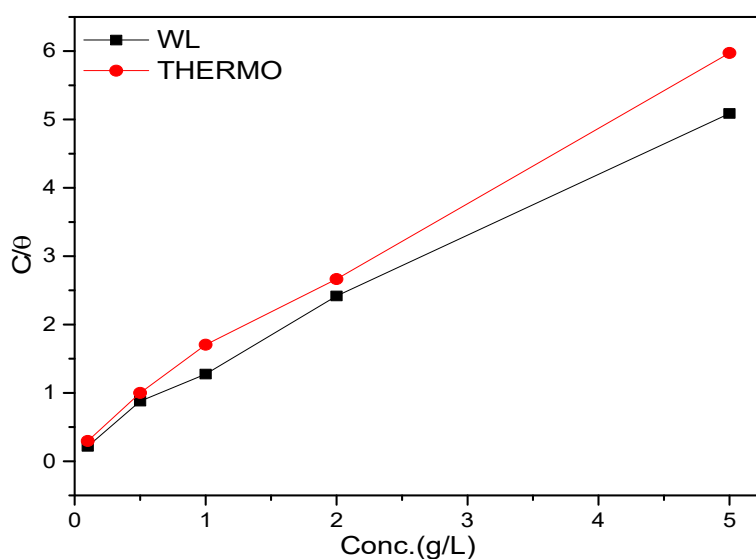


Figure 8: Langmuir’s plot of SS in a 3.5% NaCl solution with DAD various Ct, at 303 K.

The plot suggests that DAD molecules were adsorbed onto the SS surface through a monolayer process, which is one of Langmuir's isotherm assumptions. ΔG_{ads}^* was calculated using Eq. 8.

$$\Delta G_{ads}^* = -RT \ln(55.5K_{ads}) \quad (8)$$

where R is the ideal gas constant, T is 303 K, and K is the inverse of the intercept of the linear plot on the y axis.

ΔG_{ads}^* calculated for WL and thermometric methods was -13.1 and -12.5 kJ/mol, respectively. The calculated values are negative and lower than the threshold values of 40 kJ/mol. This indicates that DAD adsorption mechanism was spontaneous and physical [36-42].

Surface characterization

After 24 h of IT, the SS surface was assessed without and with DAD (5.0 g/L) using SEM technique. It is clearly seen on SEM images (Fig. 9a) that the SS surface was seriously affected in NaCl without DAD. However, with the CI, it was only slightly damaged (Fig. 9b). This revealed the formation of a film on the SS surface (via DAD molecules adsorption) [43-56].

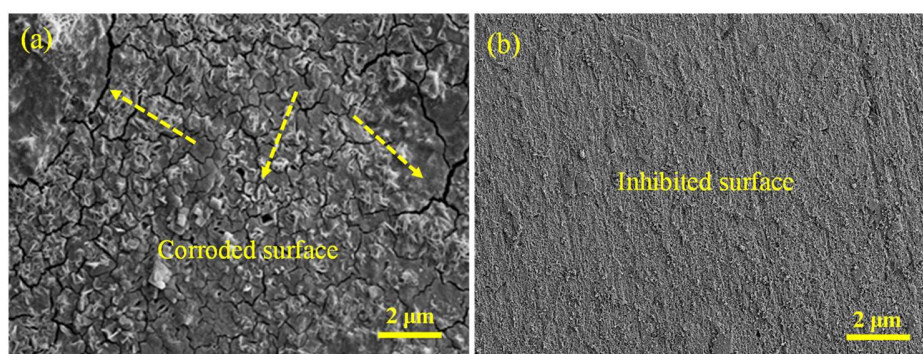


Figure 9: SEM images of SS (a) in NaCl without and (b) with DAD.

Conclusions

In this study, DAD was tested as CI of SS in a 3.5% NaCl solution. From the obtained results, the following conclusions were taken: experimental analyses indicated that DAD acted as efficient CI for SS in a 3.5% NaCl solution; thermometric measurements revealed that IE(%) increased with DAD higher Ct, at raised T; DAD adsorption onto the SS surface obeyed Langmuir's isotherm, and the mechanism was partly physical and chemical; RSM predicted CI of SS by DAD in a 3.5% NaCl solution. Error analysis revealed RSM technique superiority in modeling the CI of SS. Results from the significance test for model coefficients indicated that Ct of CI was the most important factor in SS corrosion process; and SEM analysis showed that DAD, in the optimum Ct of 5.0 g/L, at 30 °C, caused a significant reduction in the surface damage caused by the CI solution attack.

Author's tasks

Fidelis Ebunta Abeng: conceived and designed the research work; performed experimental work; wrote the draft; conducted the review before submission.

Acknowledgments

The author acknowledges the Department of Chemistry, University of Cross River State, Calabar, for offering their Physical Chemistry laboratory for this research work. He also appreciates the assistance of his students for assisting him in taking experimental measurements.

Abbreviations

ANOVA: analysis of variance
CCD: central composite design
CI: corrosion inhibition/inhibitor
Cl: chloride
CR: corrosion rate
CS: carbon steel
CV: coefficient of variation
MS: mild steel
Ct: concentration
DAD: Diaminonaphthalene azo dye
HCl: hydrochloric acid
H₂SO₄: sulfuric acid
IE(%): inhibition efficiency
IT: immersion time
MS: mild steel
NaCl: sodium chloride
NaOH: sodium hydroxide
R²: correlation coefficient
RN: reaction number
RSM: response surface methodology
SC: surface coverage (θ)
SEM: scanning electron microscopy
SS: stainless steel
STD: standard deviation
T: temperature
WL: weight loss

Symbols definition

ΔG_{ads} : adsorption free energy

References

1. Talebian M, Raeissi K, Atapour M et al. Pitting corrosion inhibition of 304 stainless steel in NaCl solution by three newly synthesized carboxylic Schiff bases. *Corros Sci.* 2019;60:108130. <https://doi.org/10.1016/j.corsci.2019.108130>
2. Sanni O, Fayomi OSI, Popoola API. Eco-friendly inhibitors for corrosion protection of stainless steel: An Overview. *J Phys.* 2019;1378:042047. <https://doi.org/10.1088/1742-6596/1378/4/042047>
3. Uwiringiyimana E, Sylvester OD, Joseph IV et al. The effect of corrosion inhibitors on stainless steel and Aluminum alloys: A Review. *Afr J Pure Appl Chem* 2016;10(2):23-32. <https://doi.org/10.5897/AJPAC2016.0676>
4. Al-Doori HH, Shihab MS. Study of Some [N-substituted] p-aminoazobenzene as Corrosion Inhibitors for Mild-Steel in 1 M H₂SO₄. *J Al-Nahrain Univer.* 2014;17(3):6859.
5. Nagiub AM, Mahross MH, Khalil HFY et al. Azo Dye Compounds as Corrosion Inhibitors for Dissolution of Mild Steel in Hydrochloric Acid Solution. *Port Electrochim Acta.* 2013;31(2):119-139. <https://doi.org/10.4152/pea.201302119>
6. Mabrouk EM, Eid S, Attia MM. Corrosion inhibition of carbon steel in acidic medium using azochromotropic acid dye compound. *J Basic Env Sci.* 2017;4:351-355.
7. Uguz O, Gumus M, Sert Y et al. Utilization of pyrazole-perimidine hybrids bearing different substituents as corrosion inhibitors for 304 stainless steels in acidic media. *J Mol Struct.* 2022;1262,133025. <https://doi.org/10.1016/j.molstruc.2022.133025>
8. Verma C, Quraishi MA, Ebenso EE et al. Amines as Corrosion Inhibitors: A Review. *Organic Corrosion Inhibitors: Synthesis, Characterization, Mechanism and Applications.* Published 2022 by John Wiley & Sons, Inc.
9. Hani ME, Bedair MA, Bedair AH et al. Synthesis, characterization of novel coumarin dyes as corrosion inhibitors for mild steel in acidic environment: Experimental, theoretical, and biological studies. *J Mol Liq.* 2022;118310. <https://doi.org/10.1016/j.molliq.2021.118310>
10. Abeng FE, Ita BI, Anadebe VC et al. Multidimensional insight into the corrosion mitigation of clonazepam drug molecule on mild steel in chloride environment: Empirical and computer simulation explorations. *Resul Eng.* 2023;17:100924. <https://doi.org/10.1016/j.rineng.2023.100924>
11. Ikeuba AI, Ntibi JE, Okafor PC, et al. Kinetic and thermodynamic evaluation of azithromycin as a green corrosion inhibitor during acid cleaning process of mild steel using an experimental and theoretical approach. *Resul Chem.* 2023;5:100909. <http://doi.org/10.1016/j.rechem.2022.100543>
12. Iroha NB, Dueke-Eze CU, Fasina TM et al. Anticorrosion activity of two new pyridine derivatives in protecting X70 pipeline steel in oil well acidizing fluid: experimental and quantum chemical studies. *J Iran Chem Soc.* 2022;19:2331-2346. <https://doi.org/10.1007/s13738-021-02450-2>

13. Maduelosi NJ, Iroha NB. Insight into the Adsorption and Inhibitive Effect of Spironolactone Drug on C38 Carbon Steel Corrosion in Hydrochloric Acid Environment. *J Bio Tribo Corros*. 2021;7:6. <https://doi.org/10.1007/s40735-020-00441-z>
14. Nkem BI, Valentine CA, Ngozi JM et al. Linagliptin drug molecule as corrosion inhibitor for mild steel in 1 M HCl solution: Electrochemical, SEM/XPS, DFT and MC/MD simulation approach. *Collo Surf A: Physicochem Eng Asp*. 2023;660:130885. <https://doi.org/10.1016/j.colsurfa.2022.130885>
15. Nkem B, Iroha, Cordelia U et al. Newly synthesized N-(5-nitro-2-hydroxybenzylidene)pyridine-4-amine as a high-potential inhibitor for pipeline steel corrosion in hydrochloric acid medium. *Egyp J Petr*. 2021;(2)30:55-61. <https://doi.org/10.1016/j.ejpe.2021.02.003>
16. Emembolu LN, Ohale PE, Onu CE et al. Comparison of RSM and ANFIS modeling techniques in corrosion inhibition studies of *Aspilia Africana* leaf extract on mild steel and aluminum metal in acidic medium. *Appl Surf Sci Adv*. 2022;11:100316. <https://doi.org/10.1016/j.rechem.2022.100543>
17. Sanni O, Adeleke O, Ukoba K et al. Application of machine learning models to investigate the performance of Stainless steel Type 904 with agricultural waste. *J Mater Res Tech*. 2022. <https://doi.org/10.1016/j.jmrt.2022.08.076>
18. Abboud Y, Abdelmjid A, Saffaj T et al. A novel azo dye, 8-quinolinol-5-azoantipyrine as corrosion inhibitor for mild steel in acidic media. *Desalination* 2009;237(1):175-189. <https://doi.org/10.1016/j.desal.2007.12.031>
19. Al-Doori HH, Shihab MS. Study of Some [N-substituted] p-aminoazobenzene as Corrosion Inhibitors for Mild-Steel in 1 M H₂SO₄. *J Al-Nahrain Univ*. 2014;17(3):59 -68. [https://doi.org/10.1016/jdesal.2007.12.031](https://doi.org/10.1016/j.desal.2007.12.031)
20. Al-Juaid SS. Mono azo dyes compounds as corrosion inhibitors for dissolution of aluminium in sodium hydroxide solutions *Port Electrochim Acta*, 2007;3:363-373. <https://doi.org/10.4152/pea.200703363>
21. Nagiub AM, Mahross MH, Khalil HFY et al. Azo Dye Compounds as Corrosion Inhibitors for Dissolution of Mild Steel in Hydrochloric Acid Solution. *Port Electrochim Acta*. 2013;31(2):119-139. <https://doi.org/10.4152/pea.201302119>
22. Fouda AS, Ali H, Awad RS et al. New BenzonitrileAzo Dyes as Corrosion Inhibitors for Carbon Steel in Hydrochloric Acid Solutions. *Int J Electrochem Sci*. 2014;9:1117-1131.
23. Mabrouk EM, Eid S, Attia MM. Corrosion inhibition of carbon steel in acidic medium using azochromotropic acid dye compound. *J Basic Envir Sci*. 2017;4:351-355.
24. Sadeq HZ, Mohammad RS. Corrosion Inhibition of Carbon Steel in Acidic Solution by Alizarin Yellow GG (AYGG). *Petro Env Tech*. 2016;5(4):1-5. <https://doi.org/10.4172/2157-7463.1000188>
25. Singh AK, Tiwari P, Srivastava S et al. Allura Red, Sunset Yellow and Amaranth Azo Dyes for Corrosion Inhibition of Mild Steel in 0.5 M H₂SO₄ Solutions. *Int J Arch Env Eng*. 2016;3(9):680.

26. Ahmed F, Arafat T. Inhibition evaluation of chromotrope Dyes for the Corrosion of Mild Steel in an Acidic Environment: Thermodynamic and Kinetic Aspects. *America Chem Soc Omega* 2021;6:4051-4061. <https://doi.org/10.1021/acsomega.0c06121>
27. Aghaaminiha MR, Mehrani M, Colahan B et al. Machine learning modeling of time-dependent corrosion rates of carbon steel in presence of corrosion inhibitors. *Corros Sci.* 2021;193:109904. <https://doi.org/10.1016/j.jcorsci.2021.109904>
28. Taylor C D, Tossey BM. High temperature oxidation of corrosion resistant alloys from machine learning. *NPJ Mat Degrad.* 2021;5(1):1-10. <https://doi.org/10.1038/s41529-021-00184-3>
29. Diao Y, Yan L, Gao K. Improvement of the machine learning-based corrosion rate prediction model through the optimization of input features. *Mat Design.* 2021;198:109326. <https://doi.org/10.1016/j.matdes.2020.109326>
30. Coelho LB, Zhang DY, Van Ingelgem D et al. Reviewing machine learning of corrosion prediction in a data-oriented perspective. *NPJ Mater Degrad.* 2022;6(1):1-16. <https://doi.org/10.1038/s41529-022-00218-4>
31. Anadebe VC, Onukwuli OD, Abeng FE et al. Electrochemical-kinetics, MD-simulation and multi-input single-output (MISO) modeling using adaptive neuro-fuzzy inference system (ANFIS) prediction for dexamethasone drug as eco-friendly corrosion inhibitor for mild steel in 2 M HCl electrolyte. *J Taiwan Inst Chem Eng* 2020;115:251-265. <https://doi.org/10.1016/j.jtice.2020.10.004>
32. Anadebe VC, Nnaji PC, Onukwuli OD et al. Multidimensional insight into the corrosion inhibition of salbutamol drug molecule on mild steel in oilfield acidizing fluid: Experimental and computer aided modeling approach. *J Mol Liq* 2022;349:118482. <https://doi.org/10.1016/j.molliq.2022.118482>
33. Bangera S, Vijaya DP, Alva VDP et al. *Hemigraphis colorata* (HC) Leaves Extract as Effectual Green Inhibitor for Mild Steel Corrosion in 1 M HCl. *Bio Interf Res Appl Chem.* 2022;2:1-23. <https://doi.org/10.33263/briac132.200>
34. Olawale O, Idefoh CK, Ogunsemi BT et al. Evaluation of Groundnut Leaves Extract as Corrosion Inhibitor on Mild Steel in 1.0 M Sulphuric Acid Using Response Surface Methodology (RSM). *Int J Mech Eng Tech.* 2018;9(11):829-841.
35. Okewale AO, Omoruwuo F, Adesina OA. Comparative Studies of Response Surface Methodology (RSM) and Predictive Capacity of Artificial Neural Network (ANN) on Mild Steel Corrosion Inhibition using Water Hyacinth as an Inhibitor. *J Phys Conf Series* 2019;1378:022002. <https://doi.org/10.1088/1742-6596/1378/2/022002>
36. Omotioma M, Onukwuli OD. Modeling the Corrosion Inhibition of Mild Steel in HCl Medium with the Inhibitor of Pawpaw Leaves Extract. *Port Electrochim Acta.* 2016;34:287-294. <https://doi.org/10.4152/pea.201604287>
37. Qiang Y, Zhang S, Guo L et al. Experimental and theoretical studies of four allyl imidazolium-based ionic liquids as green inhibitors for copper corrosion in

- sulfuric acid. Corros Sci. 2017;119:68-78. <https://doi.org/10.1016/j.corsci.2019.108193>
38. About S, Hsissou R, Erramli H et al. Gravimetric, electrochemical and theoretical study, and surface analysis of novel epoxy resin as corrosion inhibitor of carbon steel in 0.5 M H₂SO₄ solution. J Mol Struct. 2021;1245:131014. <https://doi.org/10.1016/j.molstruc.2021.131014>
 39. Baby N, Manjula P, Mainmegalai S. Azole drug: A Novel inhibitor for corrosion. Res J Chem Sci 2015;5(2):11-16.
 40. Onukwuli OD, Anadebe VC, Okafor CS. Optimum prediction for inhibition efficiency of *Sapium ellipticum* leaf extract as corrosion inhibitor of aluminum alloy (aa3003) in hydrochloric acid solution using electrochemical impedance spectroscopy and response surface methodology. Bull Chem Soc Ethio. 2020;34(1):175-191. <https://doi.org/10.4314/bcse.v34i1.17>
 41. Anadebe VC, Onukwuli OD, Omotioma M et al. Optimization and Electrochemical Study on the Control of Mild Steel Corrosion in Hydrochloric Acid Solution with *Bitter Kola* Leaf Extract as Inhibitor. South Afr J Chem. 2018;71:51-61. <http://dx.doi.org/10.17159/0379-4350/2018/v71a7>.
 42. Albo Hay Allah MA, Balakit AA, Salman HE et al. New Heterocyclic Compound as Carbon Steel Corrosion Inhibitor in 1 M H₂SO₄, High Efficiency at Low Concentration: Experimental and Theoretical Studies. J Adhesion Sci Tech. 2022;37:525-547. <https://doi.org/10.1080/01694243.2022.2034588>
 43. Abdulridha AA, Albo HAMA, Makki SQ et al. Corrosion inhibition of carbon steel in 1 M H₂SO₄ using new Azo Schiff compound: Electrochemical, gravimetric, adsorption, surface and DFT studies. J Mol Liq. 2020;315:113690. <https://doi.org/10.1016/j.molliq.2020.113690>
 44. Balaki AA, Makki SQ, Sert Y et al. Synthesis, Spectrophotometric and DFT Studies of new Triazole Schiff Bases as Selective Naked-Eye Sensors for Acetate Anion Supramolec Chem. 2020;32(10):519-526. <https://doi.org/10.1080/10610278.2020.1808217>
 45. Sathiyapriya T, Dhayalam SM, Jagadeeswari R et al. Assessing bioorganic gum performance as a corrosion inhibitor in Phosphoric acid medium: Electrochemical and computational Analysis. Mater Corros Sci. 2021. <https://doi.org/10.1002/maco.202112742>
 46. Fouda FA, El-Desoky HS, Abdel-Galeil MA et al. Niclosamide and dichlorophenamide: new and effective corrosion inhibitors for carbon steel in 1 M HCl solution. SN App Sci. 2021;3(287). <https://doi.org/10.1007/s42452-021-04155-w>
 47. Ikpi ME, Abeng FE. Electrochemical and Quantum Chemical Investigation on Adsorption of nifedipine at API 5L X-52 Steel/HCl acid interface as corrosion inhibitor. Arch Metall Mater. 2020;65(1):125-131.
 48. Anila RS, Vidya VG, Preethi V et al. Single crystal XRD and DFT investigation of 1,5-dimethyl-4-[(2-oxo-1,2-diphenylethylidene) amino]-2-phenyl-1,2-dihydro-3H-pyrazol-3-one. Resul Chem. 2022;4:100665. <https://doi.org/10.1016/j.rechem.2022.100665>

49. Mohamed MG, Mahdi A, Obaid RJ et al. Synthesis and characterization of polybenzoxazine/clay hybrid nanocomposites for UV light shielding and anti-corrosion coatings on mild steel. *J Poly Res.* 2021;28:264-276.
50. Mohamed MG, Kuo SW, Mahdi AI et al. Bisbenzylidene cyclopentanone and cyclohexanone-functionalized polybenzoxazine nanocomposites: Synthesis, characterization, and use for corrosion protection on mild steel. *Mater Today Comm.* 2020;25:101418. <https://doi.org/10.1016/j.mtcomm.2020.101418>
51. Aly KI, Mahdi AM, Hegazi A et al. Corrosion resistance of mild steel coated with Phthalimide-Functionalized polybenzoxazines. *Coating.* 2020;10:14. <https://doi.org/10.3390/coatings1011114>
52. Aly KI, Mohamed MG, Younis OM et al. Salicylaldehyde azine-functionalized polybenzoxazine: synthesis, characterization, and its nanocomposites as coatings for inhibiting the mild steel corrosion. *Prog Org Coating* 2020;138:105385. <https://doi.org/10.1016/j.porgcoat.2019.105385>
53. Hani ME, Bedair MA, Bedair AH et al. Synthesis, characterization of novel coumarin dyes as corrosion inhibitors for mild steel in acidic environment: Experimental, theoretical, and biological studies. *J Mol Liq* 2022;118310. <https://doi.org/10.1016/j.molliq.2021.118310>
54. Di Y, Li X, Chen Z et al. Experimental and theoretical insights into two fluorine-containing imidazoline Schiffbase inhibitors for carbon steels in hydrochloric acid solution. *J Mol Struct.* 2022;1268:133737. <https://doi.org/10.1016/j.molstruc.2022.133737>
55. Abeng FE, Ikpi ME, Ushie OA et al. Insight into corrosion inhibition mechanism of carbon steel in 2 M HCl electrolyte by eco-friendly based pharmaceutical drugs. *Chem Data Collec.* 2021;34:100722. <https://doi.org/10.1016/j.cdc.2021.100722>
56. Abeng FE, Anadebe VC, Nkom PY et al. Experimental and theoretical study on the corrosion inhibitor potential of quinazoline derivative for mild steel in hydrochloric acid solution. *J Electrochem Sci Eng.* 2021;11:11-26. <https://doi.org/10.5599/jese.887>